LAWRENCE
LIVERMORE
NATIONAL
LABORATORY

LLNL-TR-812018

A Mercury Model of the Molly-G Fast Burst Reactor (FBR)

R. J. Procassini

June 25, 2020

Disclaimer

This work performed under the auspices of the U.S. Department of Energy by Lawrence Livermore National Laboratory under Contract DE-AC52-07NA27344.

A Mercury Model of the Molly-G Fast Burst Reactor (FBR)

Richard 'Spike' Procassini
Design Physics Division

15 June 2020

1 Introduction

In order to design neutron irradiation experiments at a given nuclear reactor, one requires a representative neutron spectrum for the configuration of the reactor that will exist during the experiment. This usually implies modeling the operation of the reactor using a neutron transport code. Since the modeling of pulsed neutron reactors is quite complex, requiring coupled modeling of neutronics and thermo-structural response, the typical methodology employs analysis of the neutron spectrum which is obtained from a static k_{eff} calculation. While this time-independent Eigenfunction is not truly representative of that during a reactor pulse, we postulate that it is a reasonable representation for our purposes.

The Nuclear Survivability (NS) Program at LLNL is considering fielding such experiments at the Molly-G ('Molybdenum Godiva-II') Fast Burst Reactor (FBR) at the White Sands Missile Range (WSMR). The goal of these experiments is to (a) test / proof / calibrate diagnostics, and (b) test the efficacy of neutron shield configurations, before fielding at other nuclear reactors, such as the Annular Core Research Reactor (ACRR) at SNL/NM. After attempting to secure either drawings or a copy of an existing ***MCNP*** model of the Molly-G FBR from various institutions, it was decided to develop a new model for use with the ***Mercury*** Monte Carlo transport code. The model described herein will be used to design these experiments.

2 Re-engineering the Reactor Model

When developing a computational model which will be used in the design of neutron irradiation experiments, one either (a) starts with a set of drawings / sketches for the various components in order to define the geometry, material composition, and density / mass of the parts, or (b) starts with an existing computational model, typically for use with another code, and translates it into the code of choice. For the Molly-G FBR, neither of these options was possible. Therefore, the ***Mercury*** model was re-engineered from all available sources of information.

For this particular computational model, the sum total of information that was drawn from a variety of technical reports, meeting presentations and online facility 'brochures', was not sufficient to fully define the model. As a result, a number of assumptions were made to complete the definition of the model. These assumptions will be highlighted below. While one might believe that making such assumptions will produce a model that is not useful for the stated purpose, the validation of the model (presented in the following section) against experimental data and simulations performed with other codes will demonstrate that the model is, indeed, sufficient for our purposes. That is not to say that the model could not be improved. On the contrary, the model will undergo continual improvement if and when additional facility information becomes available.

The bulk of the ***Mercury*** model has been developed based upon the information defined in a technical review report [1], a master's dissertation [2], and two presentations from scientific conferences [3, 4]. Many of the original documents that describe the facility were not available online. The chosen documents span more than 5 decades, and were written by authors at

various institutions. The final references were invaluable for validating the ***Mercury*** model against available experimental data and results from previous modeling efforts.

The bulk of the ***Mercury*** model of the Molly-G FBR was derived from the following paragraphs and associated cutaway sketch [1]:

> <u>*Molly-G*</u>
>
> *The White Sands Missile Range (WSMR) Fast Burst Reactor was designed and developed by Kaman Nuclear, a subsidiary of Kaman Aircraft Corporation, with the exception of the core which was designed by WSMR engineering staff with consultation services supplied by Los Alamos Scientific Laboratory and Sandia Corporation. The core, illustrated in Figure* **1***, is similar to HPRR* (the Health Physics Research Reactor, which became the Bare Reactor Experiment Nevada [BREN])) *in its cylindrical shape and use of the U-10 w/o Mo alloy. To satisfy requirements for irradiation applications, the core is mounted on a small stand similar to that of Godiva-II or SPR-I (thus its nickname 'Molly-G' for molybdenum-alloy Godiva). The portable stand is normally fastened to a hydraulic lift which is used to lower the assembly into a pit beneath a shield (as in SPR-I) inside a large reactor building, otherwise the assembly may be transported readily on a fork lift to an outdoor site for free space experiments. The core as shown in Figure* **1** *Is 8 inches in diameter and 7 5/8 inches high.*
>
> *The safety block is ~4 inches in diameter and 5 3/4 inches long with a stainless steel core 1.25 inches in diameter, and its withdrawal reduces reactivity by ~30$. The total weight of U-Mo is ~97 kg in this configuration. Reactivity control is accomplished by the usual two control rods and a burst rod (~1.5$ each) and, in addition, there is provision for step-wise adjustments of ~ one dollar by means of a mass-adjustment or shim ring shown at the top of the core in the figure. For example, a shim ring of iron adds ~ one dollar, while one of U-Mo adds ~ three dollars in reactivity. The fuel rings are bolted together and to the support plate by three 3/4-inch bolts. Those shown in the drawing and currently in use are made of a special high-strength nickel alloy, Inconel X, which exhibits a yield strength of ~180,000 psi.*

Again, this is not sufficient to develop a high confidence model, but it is a very good start. Of course, the goal is to produce a reasonable computational model of the reactor, not an exact replica. Therefore, a number of features that are shown in Figure 1 are not included in the model, namely the retaining plate, vent holes, thermocouple holes, air flow grooves, assembly steps in the fuel rings, and control element drive rods. The dimensions of many components were not provided in the description above. Therefore, they were 'measured' off of the figure. These include the radii of the center insert and mass adjustment ring, radius and thickness of the support plate, and radius and length of the control and burst rods. Additional dimensions were derived based upon fuel mass constraints, including the outer radius of the safety block, and the inner radius of the lower rings $\left(r = 2.0\ inch\right)$.

In the end, the resulting model was fairly accurate in terms of the total fuel mass, and validation against the experimental data (see the following section). The individual fuel part volumes and masses in the ***Mercury*** model are shown in Table 1. The U-10Mo fuel mass of the Molly-G FBR, as shown in Figure 1, is stated to be $m_{U-10\,Mo} \sim 97\ kg$ [1]. For this particular configuration, the model fuel mass is $m_{U-10\,Mo} = 97144.77\ g$. If the mass adjustment ring (MAR) is made of U-10Mo, the total fuel mass becomes $m_{U-10\,Mo} = 99660.35\ g$.

Images of the ***Mercury*** model of the Molly-G FBR, color coded by the material comprising each part, are shown in Figure 2. Figure 2a is an outer view of the complete reactor, while Figure 2b is the same view, but with the top and bottom fuel rings removed. Additional components that are not visible include the (7) second control rod (U-10Mo_E), (10) center plug

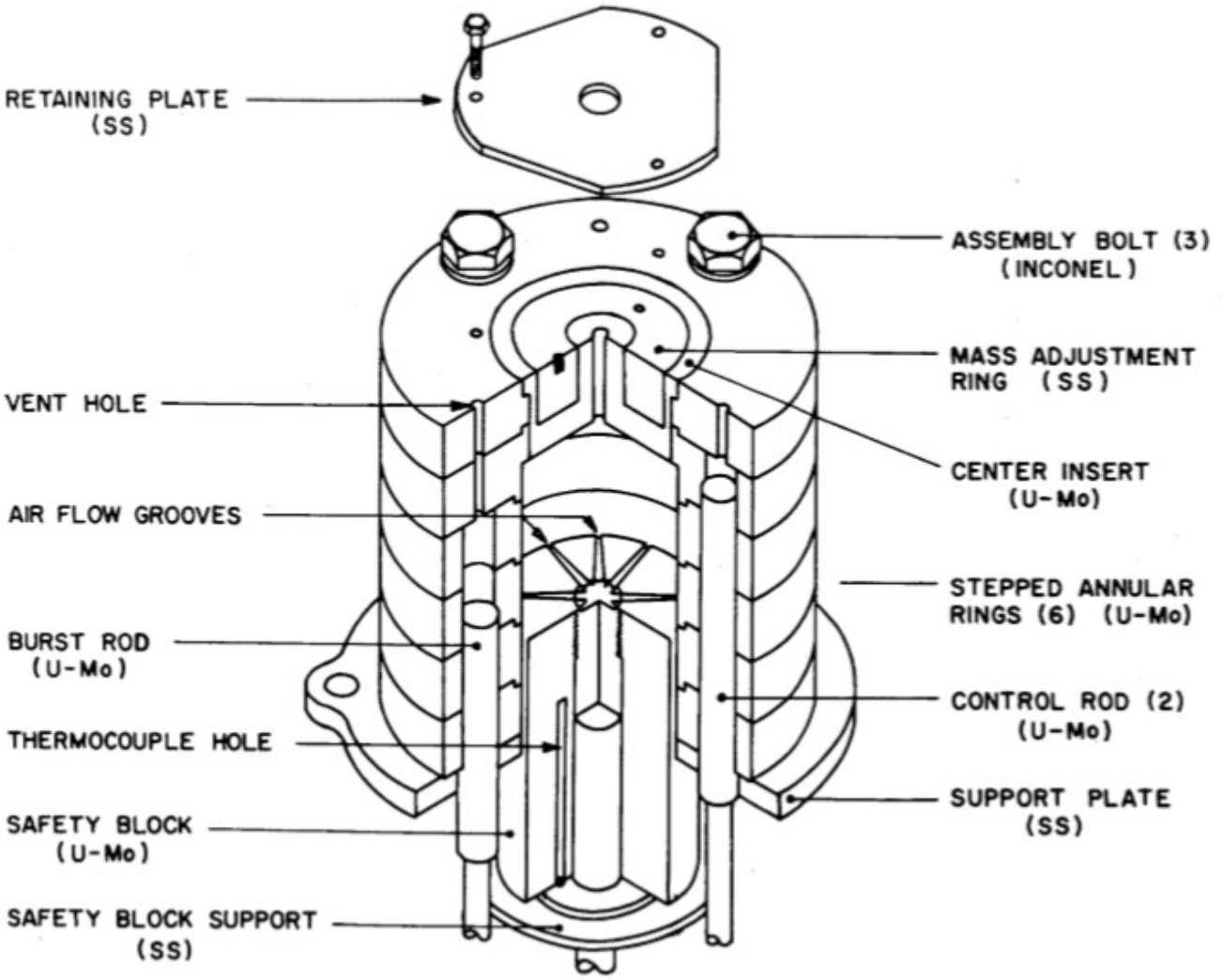

Figure 1. Cutaway sketch of the Molly-G Fast Burst Reactor (FBR).

*Table 1. Molly-G **Mercury** Model Fuel Part Volumes and Masses*

Part	***Volume [cm^3]***	***Mass [g]***
Top Rings (L = 1.87 in)	1164.32	19909.87
Bottom Rings (L = 5.75 in)	3263.95	55813.55
Safety Block	897.49	15347.08
Center Insert	180.02	3078.34
Mass Adjustment Ring	147.11	2515.58
Control Rod (x 2)	62.57	1069.95
Burst Rod	50.06	856.03
Total	*5827.09*	*99660.35*

When the U-10Mo mass adjustment ring (MAR) is replaced by a stainless steel MAR, the total U-10Mo fuel mass in the Molly-G FBR is 97144.77 g.

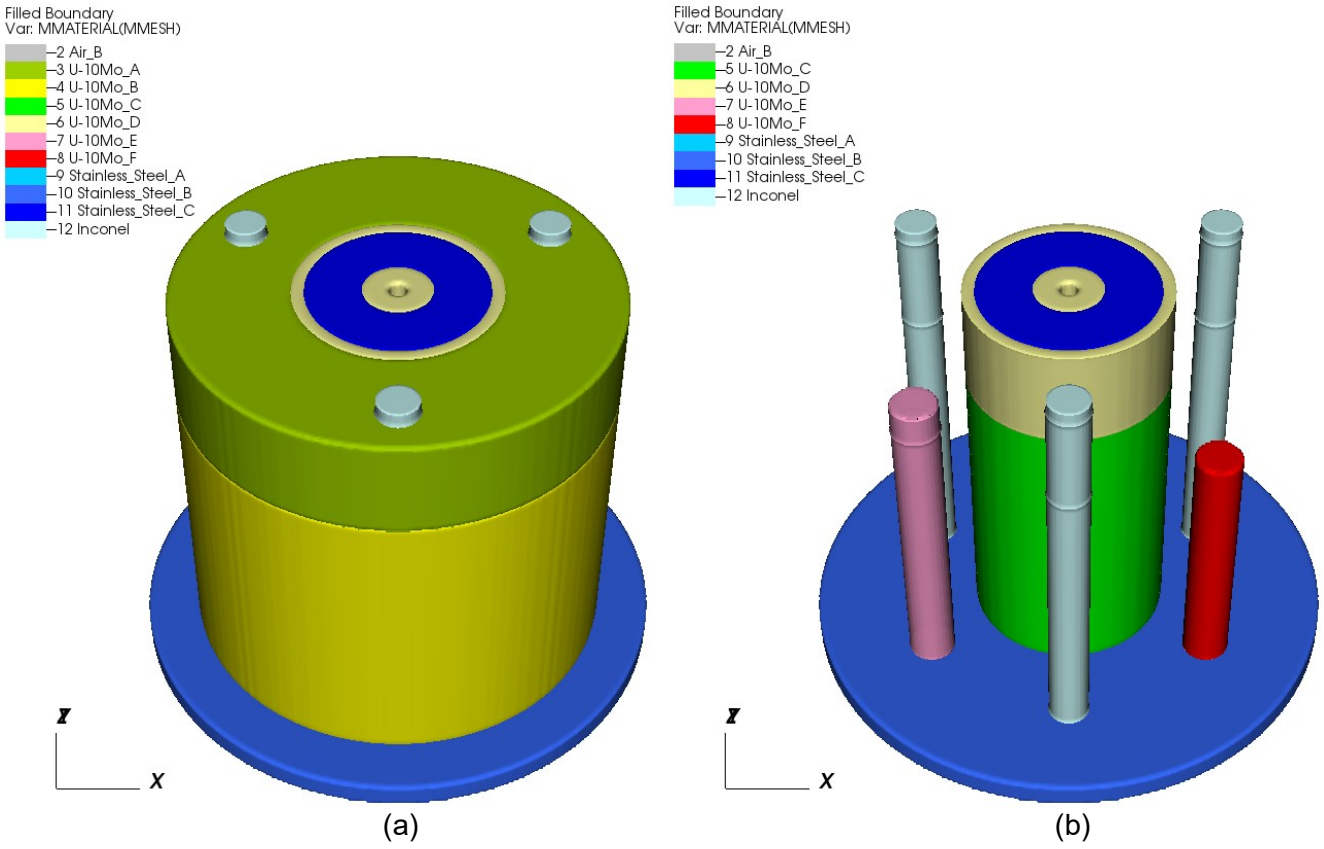

Figure 2. ***Mercury*** model of the Molly-G Fast Burst Reactor (FBR): (a) the complete model of the FBR code, and (b) the same view, but with the top and bottom fuel rings removed. The components of the FBR that are shown in the images include the (1) top fuel rings (U-10Mo_A), (2) bottom fuel rings (U-10Mo_B), (3) safety block (U-10Mo_C), (4) center inset (U-10Mo_D), (5) two control rods [one is visible] (U-10Mo_E), (6) burst rod (U-10Mo_F), (7) support plate (Stainless_Steel_B), (8) mass adjustment ring (Stainless_Steel_C), and (9) assembly bolts (Inconel).

(Stainless_Steel_A), and (11) the fuel mass adjustment ring (U-10Mo_G) which would replace the stainless steel version (8) shown

A different view of the Molly-G FBR core is shown in Figure 3. Here, the control elements are each partially withdrawn out of the core downwards through the support plate. The burst rod (U-10Mo_F) is withdrawn 3 cm, control rod 'A' (U-10Mo_E) is withdrawn 5 cm, and control rod 'B' (U-10Mo_E) is withdrawn 7 cm. The model has been parameterized to support independent withdrawal of each of the control element up to the fully withdrawn position (12.91 cm for the burst rod, and 16.19 cm for each control rod. In addition, the mass adjustment ring (MAR) may be removed, or either a stainless steel or U-10Mo fuel MAR may be included. The ability to control the location and/or inclusion of the control elements and shim rings will be used to assess the worth of each component in the following section.

The fuel is composed of 90 weight percent HEU mixed with 10 weight percent molybdenum. Since (a) the enrichment of ^{235}U in the HEU fuel is not provided, and (b) it is mentioned that Molly-G is similar to the Health Physics Research Reactor (HPRR) (also known as the Bare Reactor Experiment Nevada or BREN), it was assumed that the enrichment of Molly-G fuel is the same as that in HPRR / BREN (93.17%) [5]. The isotopic composition of the minor ura-

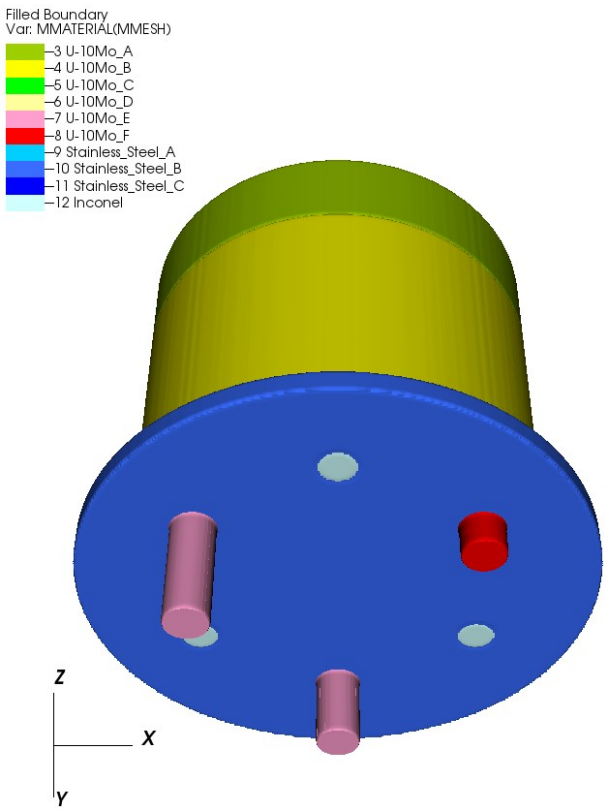

Figure 3. ***Mercury*** model of the Molly-G Fast Burst Reactor (FBR) with the control elements partially withdrawn from the core: (a) the burst rod (U-10Mo_F) withdrawn 3 cm, (b) control rod 'A' (U-10Mo_E) withdrawn 5 cm, and (c) control rod 'B' (U-10Mo_E) withdrawn 7 cm.

nium isotopes is assumed to scale in accordance with Godiva-I HEU fuel based upon its ^{235}U content. Therefore, the atom fractions of the uranium isotopes are ^{234}U: 1.11×10^{-2}, ^{235}U: 9.317×10^{-1}, and ^{238}U: 5.72×10^{-2}. The isotopic composition of the molybdenum is assumed to be the naturally occurring abundances. The isotopic composition of the remaining materials have been either taken directly, or derived from, the information found in the PNNL material compendium [6]. The stainless steel composition is a simplified average of Types 304 and 316, the aluminum parts are assumed to be pure ^{27}Al, concrete is the NIST standard, and the borated gypsum is assumed to be 10 weight percent boron in gypsum.

The balance of the facility is less well defined than the core of the FBR. A recent paper [4] on the exposure cell containing the Molly-G FBR says:

> *The assembly is operated in a 15.2 by 15.2 by 6.1 meter exposure cell constructed of thick concrete walls lined by gypsum and borated gypsum wall-board. The wall, floor, and ceiling neutron return component adds a 1/E tail to the primary fission leakage component.*

While this is helpful, it is not a complete description. How thick are the concrete walls, ceiling and floor? (They are assumed to be 2 feet thick). What is the composition of the concrete? (It is assumed to be the NIST standard). How thick are the gypsum and borated-gypsum wall boards? (They are each assumed to be 0.5 inch thick). Where is the wall board located? (It is assumed to cover the walls and ceiling of the exposure cell).

While it is mentioned [4] that the FBR is raised out of a storage vault under the concrete floor a stand, there is no detailed description or drawing to work from (although low-resolutions pho-

tos of the reactor mounted on the stand do exist). Similarly, it is mentioned [4] that an experimental table is provided to place experimental packages onto. However, no description, drawing or photo is available to aid in model development.

Finally, it is mentioned [7] in passing that a shroud is placed over the core to ensure at least minimal spacing between the outer radius of the core and experimental packages that could alter the reactivity of the core if the package was permitted to contact the core:

> *In normal operating mode, the core is surrounded by a boron-10 lined aluminum shroud.*

However no information is provided on the shroud geometry, or ^{10}B material composition. Therefore, much of the design of the shroud had to be assumed. This includes a $\Delta r(B_4C) = 1\ mm$ thick layer of boron carbide (natural ^{10}B enrichment) that is placed inside of an aluminum cylindrical 'can' housing of thickness $\Delta r(Al) = 4\ mm$. The inner radius of the boron carbide is $r_i(B_4C) = 10.66\ cm$ with a radial air gap of $\Delta r(Air) = 5\ mm$ between the outside of the core and inside of the boron carbide. The bottom of the shroud end cap is assumed to sit on the top of the assembly bolt heads (although [4] indicates that the should extends ~ 6 cm above that height).

3 Model Validation

Validation of the ***Mercury*** model of the Molly-G FBR entails comparison of experimental data against simulated results. Some of the data is quite detailed (radial, axial and angular variation of neutron fluence in the vicinity of the reactor core; simulations of the neutron spectrum as a function of distance from the core), while other data is rather approximate (worth of control elements and shim rings quoted above). Comparisons with the approximate data is provided first, followed by comparisons to radially, axially and angular varying data, and finish up with comparisons to spectra data.

3.1 Control Element and Shim Ring Worth

The ***Mercury*** model does not permit movement (and hence worth) of the safety block. However, it does permit movement of control elements and substitution of various shim rings. The worth values provided in [1] are rather approximate, but do permit one to assess reasonable validity of the model. The comparison of the experimental and simulation component worths are shown in Table 2.

For the shim rings, the worth is based upon the difference in k_{eff} between the ring inserted and the ring removed (air or void). As can be seen in Table 2, the computed shim ring worths are about 25 cents higher than the approximate experimental values given in [1]. This difference is reasonable, based upon the rather approximate nature of the experimental values provided.

For the control elements, the worth is based upon the difference in k_{eff} between the specified component fully withdrawn, and all control elements fully inserted. These calculations are performed for each shim ring material: air (void), stainless steel and U-10Mo. At first glance, the quoted [1] control and burst rod worths (~$1.5) seem strange, based upon the fact that the burst rod is about 20% shorter than the control rods. Hence, the quoted reactivity value of ~$1.5 is truly not reliable beyond the statement that $1 ~ $1.5. In contrast, the simulated rod worths actually indicate that the control rods are worth ~15 – 24% more than the burst rod, depending upon shim ring material.

Table 2. Molly-G Shim Ring and Control Element Worths

Shim Rings

Shim Ring Material	***Exp Worth [$]***	***Sim k_{eff}***	***Sim Worth [$]***
Air (void)	-	1.018151 +/- 1.88x10^{-4}	-
Stainless Steel	~1	1.026735 +/- 2.01x10^{-4}	1.26
U-10Mo	~3	1.040678 +/- 1.99x10^{-4}	3.23

Control Elements

Control Element	***Exp Worth [$]***	***Length Withdrawn [cm]***	***Sim k_{eff}***	***Sim Worth [$]***
Shim Ring: Air (void)				
Control Rod	~1.5	12.91	1.011563 +/- 1.95x10^{-4}	-0.98
Burst Rod	~1.5	16.13	1.010087 +/- 1.81x10^{-4}	-1.21
Shim Ring: Stainless Steel				
Control Rod	~1.5	12.91	1.020227 +/- 1.91x10^{-4}	-0.96
Burst Rod	~1.5	16.13	1.019211 +/- 1.91x10^{-4}	-1.11
Shim Ring: U-10Mo				
Control Rod	~1.5	12.91	1.034029 +/- 1.90x10^{-4}	-0.95
Burst Rod	~1.5	16.13	1.032670 +/- 2.01x10^{-4}	-1.15

3.2 *Radial, Axial and Angular Variation of Neutron Fluence*

The neutron fluence in the vicinity of the Molly-G FBR core was measured via activation of sulfur pellets which were placed at a variety of radii, height and angles relative to the core centerline, core bottom and reference angle. The neutron-induced reaction ^{32}S (n, p) ^{32}P in sulfur is a threshold reaction for neutrons with energies $E_n > 3\ MeV$. It is a standard means of measuring the high neutron fluence in nuclear facilities.

A comparison of the radial dependence of the experimental and ***Mercury*** simulated neutron fluence is shown in Figure 4. The simulated results were normalized to the experimental data at $r = 15.24\ cm$. Although the agreement is quite good, it is clear that the simulated results are slightly larger than the experimental data. The is especially true at larger distances from the core center line, which might be indicative of an issues in the definition of the exposure cell walls / ceiling / floor (geometry and/or material composition).

The axial (height) variation of the experimental and ***Mercury***-simulated neutron fluence at two angular locations are compared in Figure 5. The two locations are on opposite sides of the reactor: one adjacent to a control rod (blue markers) and one adjacent to an assembly bolt (red markers). The experimental data is represented by the dots, while the simulated results are represented by the plus signs. The simulated neutron fluence near the core midplane $(z = 8.89\ cm)$, in the vicinity of the control rod, is normalized to the experimental value. Although the general shape of the axial dependence of the fluence is in general agreement between experiment and simulation (peaks at the core midplane, falling off both above and below) there appears to be irregular variability from point to point in the

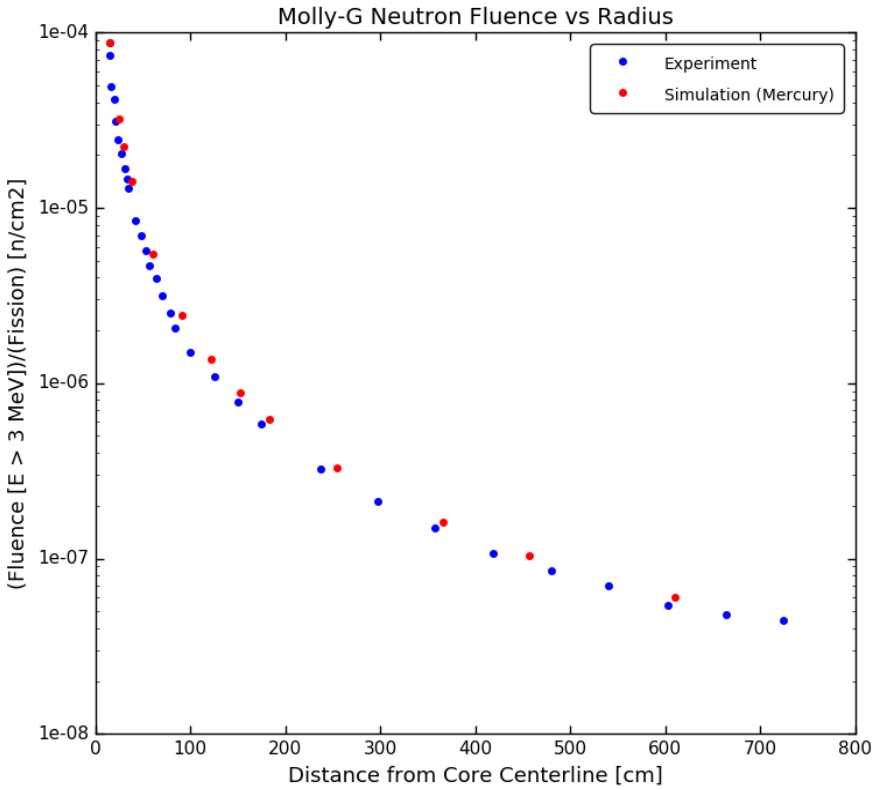

Figure 4. Comparison of the radial dependence of the experimental (blue dots) [4] and ***Mercury***-simulated (red dots) neutron fluence (MAR Material: stainless steel).

Figure 5.

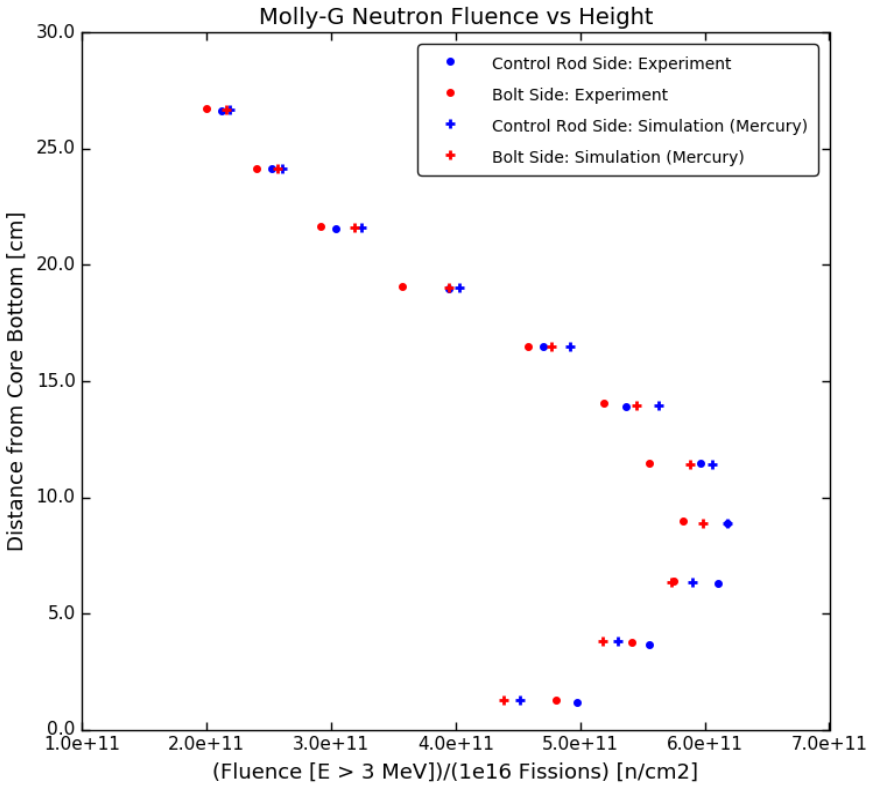

Comparison of the axial (height) dependence of the experimental (dots) [4] and ***Mercury***-simulated (plus signs) neutron fluence at two angular locations (MAR Material: stainless steel).

simulated results, and to a lesser degree, the experimental data. In addition, the experimental side-to-side (rod-to-bolt) differences are larger than their simulated counterparts, especially near the core midplane. The good news is that both the experimental data and simulated results in the vicinity of the assembly bolt are uniformly lower than the values of the fluence at the same height in the vicinity of the control rod, as expected. Unfortunately, there is a pronounced reduction in the simulated neutron fluence relative to the experimental data for heights below the core midplane. This is a consequence of the model not including the reactor stand and experimental table. Therefore, the near-field scattering provided by these features does not occur in the simulations, resulting in markedly lower fluences at the lowest heights than what is measured. This shortcoming of the model must be addressed, since our experiments will be designed and placed at the smallest available radius , with diagnostics that extend below the core midplane.

A comparison of the angular dependence of the experimental and ***Mercury***-simulated neutron fluence is shown in Figure 6. The angular-average of the simulated results were normalized to the angular-average of the experimental data. A sinusoidal variation of the neutron fluence is clearly visible in the simulated results, and to a lesser degree, in the experimental data. This variation is a consequence of the periodic angular placement of the assembly bots and control / burst rods within the core. The neutron fluence is suppressed in the vicinity of the assembly bolts $(\theta = 30^o\ ,\ 150^o\ ,\ 270^o)$, and enhanced in the vicinity of the control rods $(\theta = 90^o\ ,\ 210^o\ ,\ 330^o)$ (see Figure 2a). Angles are measured relative to the *x*-axis. The variation in the experimental data between neighboring extrema is larger in the experimental data than it is in the simulated results (which look extremely regular).

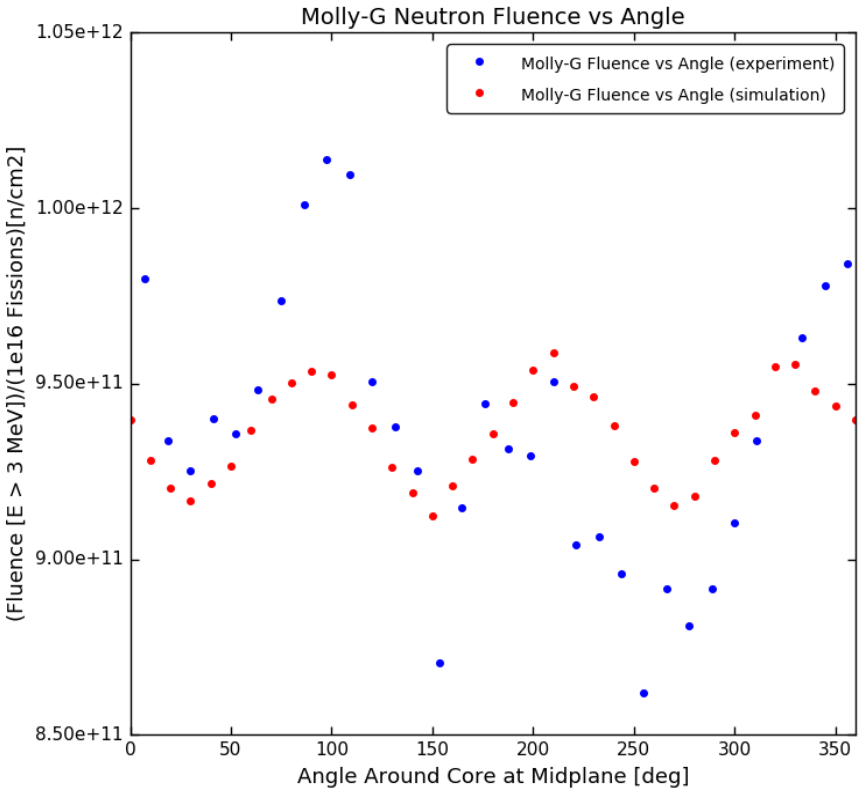

Figure 6. Comparison of the angular dependence of the experimental (blue dots) [4] and ***Mercury***-simulated (red dots) neutron fluence around the core at the midplane. The neutron fluence is suppressed in the vicinity of the assembly bolts , and enhanced in the vicinity of the control rods (MAR Material: stainless steel).

3.3 *Neutron Spectral Quantities: Energy Fluence and Spectral Index*

Simulated neutron energy-fluence spectra at various distances from the core centerline are compared in Figure 7. Figure 7a shows results from ***MCNP*** [4], while Figure 7b are the results from ***Mercury***. The agreement between the simulated results is very good to excellent, especially at smaller distances from the core centerline. At larger distance, the ***MCNP*** results exhibit larger energy fluences at low-to-moderate particle energies $\left(E_n < 1\times10^{-3}\ MeV\right)$ than do the ***Mercury*** results. The ***Mercury*** calculations were run with a modest number of particle histories (70 minutes run time on 20 processors): 250 K particles per each of 2975 k_{eff} iterations for a total of 743.75 M particle histories. Based upon the level of stochastic noise in the ***Mer-***

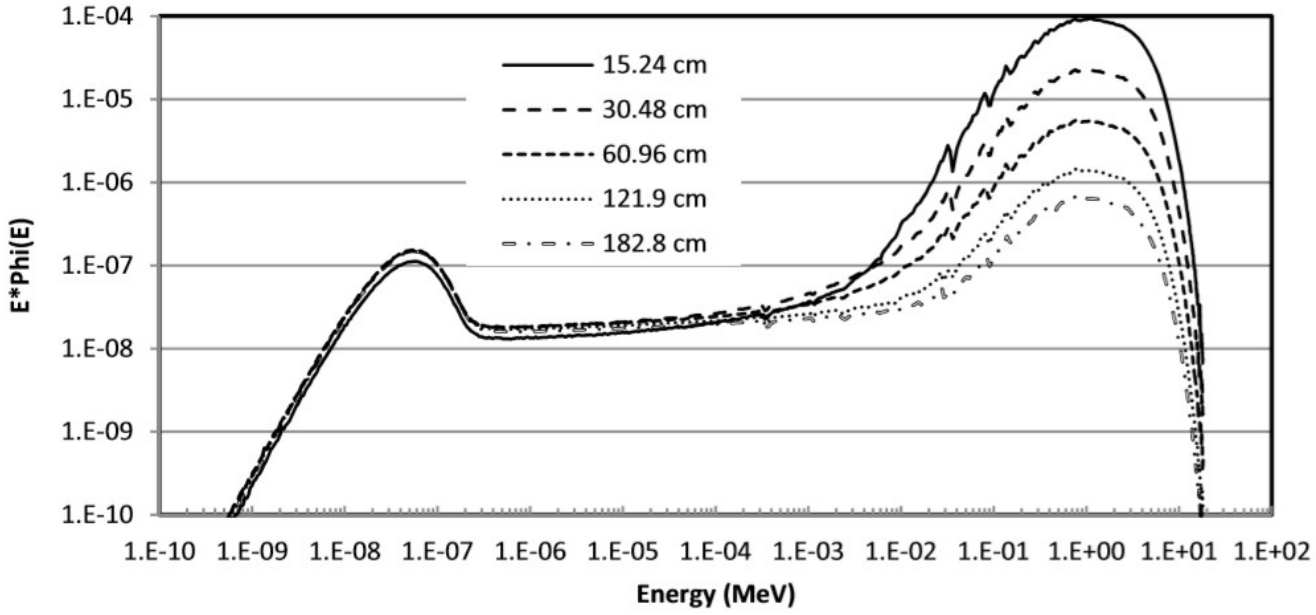

(a)

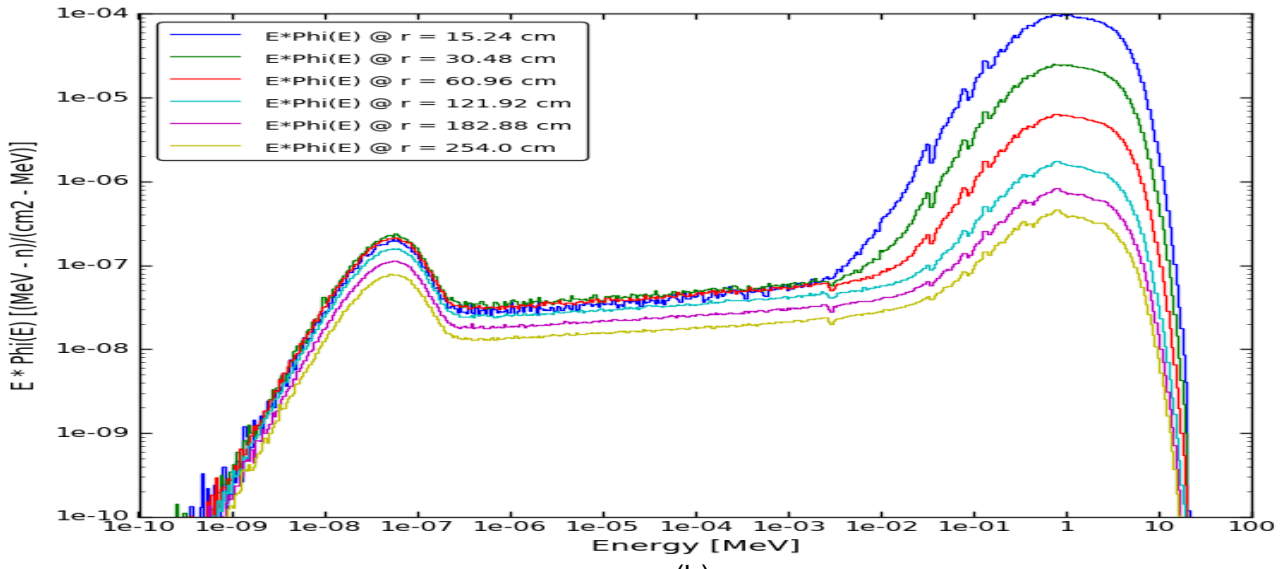

(b)

Figure 7. Comparison of the simulated neutron spectra at various distances from the core centerline: (a) ***MCNP*** results [4], (b) ***Mercury*** results (MAR Material: stainless steel).

cury results, especially at low neutron energies, it is surmised that the ***MCNP*** calculations were run with on the order of 10^{11} particle histories.

The spectral index is an important parameter that provides a means of comparison of relative spectral shapes. It is directly measurable by the relative activation of different sets of fluence monitors (activation foils). It has been used to characterize the neutron spectrum at various distances from the Molly-G FBR core centerline for years[4]. It is defined as:

$$\left(\zeta = \frac{\int_0^{\infty} \Phi(E)\,dE}{\int_{3\ MeV}^{\infty} \Phi(E)\,dE} \right)$$

Table 3 presents a comparison of experimental and simulated spectral indices at a variety of distances from the Molly-G core centerline [4]. The simulated results are obtained from both ***MCNP*** and ***Mercury*** calculations. As the distance from the core centerline increases, the spectral index is found to increase, indicating a relative 'softening' of the neutron spectrum. This is likely a result of neutrons, born in the core, which are are down scattered by the wall / ceiling / floor of the exposure cell, as well as the reactor stand and experimental table, before they interact with the activation foils. At a given distance, the simulated results are larger than the experimental data. Furthermore, the ***Mercury*** results are larger than those from ***MCNP***. Although differences in nuclear cross sections might explain these differences, it is more likely that neither computational model of the environment outside the FBR core is accurate. Based upon the assumptions made (exposure cell geometry and composition), and lack of emplacement information (no stand or experimental table), it is not surprising that the ***Mercury*** results do not agree all that well with the experimental data are larger stand-off distances.

4 Summary

A computational model of the Molly-G FBR and environment has been developed for use with the ***Mercury*** Monte Carlo particle transport code. This model is intended for use in the design of neutron irradiation experiments at the WSMR facility. Development of the model was complicated by a severe lack of facility design and construction information. Detailed drawings are not generally available to the public. As a result, information from a variety of sources was gathered, and cobbled together with several inferences and assumptions, to create a model that has been demonstrated to perform reasonably well at close stand-off distances from the core centerline. Additional information about the design and construction of the facility (beyond the core itself) will be required in order to improve the model further.

Table 3. Spectral Index at Various Distances from the Molly-G Core Centerline

Distance from Core Centerline [cm]	***Exp ζ***	***Sim ζ (MCNP)***	***Sim ζ (Mercury)***
15.24	7.85	7.86	7.80
30.48	-	-	7.91
60.96	8.02	8.20	8.37
121.92	8.63	9.14	9.78
182.88	-	-	11.01
254.0	12.0	12.0	12.11

Mass Adjustment Ring Material: stainless steel

The model has been validated against several types of experimental data, as well as previous simulations using ***MCNP***. The model gave reasonable matches to the integral shim-ring and control-element worth data, considering the approximate nature of the experimental data quoted. In most cases, the agreement between the ***Mercury*** simulations and data were good when comparing the radial, axial and angular variation of the neutron fluence. A similar level of agreement was observed when comparing ***Mercury*** results to both data and ***MCNP*** results for neutron spectra and spectral index quantities. In general, the level of agreement fell off at either larger distances from the core centerline, or at locations below the core midplane. This is directly attributable to the lack of information on the environment surrounding the FBR core. While this limitation will need to be corrected before final experiment design calculations can be performed, the model, as it currently exists, is suitable to start the design process.

References

[1] Wimett, T. F., 'Fast Burst Reactors in the United States of America', in proceedings *IAEA Symposium on Pulsed Neutron Methods*, Karlsruhe, Germany, and Los Alamos National Laboratory technical report LA-DC-6786 (1965).

[2] Schulmeister, T. R., 'Modeling the White Sands Missile Range Fast Burst Reactor Using a Discrete Ordinates Code (PENTRAN)', Air Force Institute of Technology Master's Thesis (2017).

[3] Flanders, T. M., Sparks, M. H. and Daniel, J. D., 'Highly Perturbed Operational Test Configurations at the WSMR Fast Burst Reactor', EPJ Web of Conferences **106**, 01007 (2016).

[4] Sparks, M. H. and Flanders, T. M., 'A Re-Evaluation of the Reference Environment at the WSMR Fast Burst Reactor', EPJ Web of Conferences **106**, 01006 (2016).

[5] Lundin, M. I., 'Health Physics Research Reactor Hazards Summary', Oak Ridge National Laboratory technical report ORNL-3248 (1962).

[6] McConn, Jr., R. J., Gesh, C. J., Pagh, R. T., *et al.*, 'Compendium of Material Composition Data for Radiation Transport Modeling', Pacific Northwest National Laboratory technical report PNNL-15870 (Revision 1) (2011).

[7] National Technical Information Service (NTIS), 'Federal Laboratory and Technology Resources (5th Edition)', p. 397 (1993).

Disclaimer